Why curved wind turbine rows are better than straight ones

Krabben, I. G. W.; van der Laan, M. P.; Koivisto, Matti Juhani; Larsen, Torben J.; Pedersen, M. M.; Hansen, K. S.

Published in:
Proceedings of the Wake Conference 2019

Link to article, DOI:
10.1088/1742-6596/1256/1/012028

Publication date:
2019

Document Version
Publisher's PDF, also known as Version of record

Why curved wind turbine rows are better than straight ones

IOP Conf. Series: Journal of Physics: Conf. Series **1256** (2019) 012028 doi:10.1088/1742-6596/1256/1/012028

Why curved wind turbine rows are better than straight ones

I G W Krabben[1], M P van der Laan[2], M. Koivisto[2], T J Larsen[2], M M Pedersen[2], and K S Hansen[3]

[1]University of Twente, Department of Thermal and Fluid Engineering, 7500 AE Enschede, The Netherlands
[2]Technical University of Denmark, DTU Wind Energy, Risø Campus, DK-4000 Roskilde, Denmark
[3]Technical University of Denmark, DTU Wind Energy, Lyngby Campus, DK-2800 Kgs. Lyngby, Denmark

E-mail: plaa@dtu.dk

Abstract. Wind turbine wake effects in wind farms not only reduce the wind farm power production but also influence the wind farm power dependency on wind direction. In this paper, the wake effects in wind farm layouts consisting of curved and straight wind turbine rows are studied using engineering wake models and a Reynolds-averaged Navier-Stokes model. These models predict a similar annual energy production for both wind farm layouts, but show stronger wake losses in the aligned wind directions for a rectangular wind farm layout, while the wake losses for a curved wind farm layout are more spread out over a larger wind direction sector. An energy system level simulation predicts that the enhanced spreading of wake losses over wind directions results in less hourly variability in energy generation on a Danish energy system level. Thus, our results show that a curved wind farm layout is more favorable compared to a wind farm layout with straight rows.

1. Introduction

The global cumulative offshore wind energy capacity has increased exponentially over the last decade and is expected to further increase in order to reduce the need of CO_2 producing energy sources [1]. Hence, offshore wind energy is going to be increasingly important in the energy supply and demand. From an energy system point of view, fluctuations in wind energy generation are associated with costs, mainly when the energy demand is higher than the energy supply because additional generation of energy is required [2]. The energy output of a wind farm mainly depends on the wind speed, but energy losses due to wake effects [3], which depend on wind speed, wind direction and wind farm layout, also affect the energy output. These factors are contributing to a fluctuating energy supply to the electricity grid. Feng et al. [4] included the power variability in a wind farm layout optimization, which resulted in irregular wind farm layouts. In this paper, the wake losses in wind turbine layouts with curved and straight rows are investigated. We show that the energy production of wind farm layouts with straight rows is more dependent on wind direction than the production of wind farms with curved layouts. Additionally, we observe the effect of wind direction dependency on an energy system level.

As of December 2018, in Denmark 13 offshore wind farms are established and one is

under construction, see Figure 1 (Vindeby, the world's first offshore wind farm, has been decommissioned in 2017). There is an existing trend of building wind farms in a curved layout. Among the Danish wind farms, examples of recently built curved wind farms are Middelgrunden (2000, designed curved because of architectural reasons), Horns Rev II (2009), Rødsand II (2010) and Anholt (2013). One possible reason for building curved wind farms is due to foundation costs, which increase with sea depth. Offshore wind farms are often constructed on top of reefs and wind turbine rows also do often follow the curved reef edges or sea depth contours. Sea depth data from EMODnet [5] is used in a seabed contour analysis for the wind farms mentioned above and shows that the Rødsand II and Anholt wind farm layouts have some alignment with the contours of the seabed, as shown by Figure 2. However, this is not the case for the Horns Rev II wind farm. In the present work, the wake effects of the Horns Rev II wind farm are studied to investigate if an increase in annual energy production (AEP) is the reason for building curved wind farms.

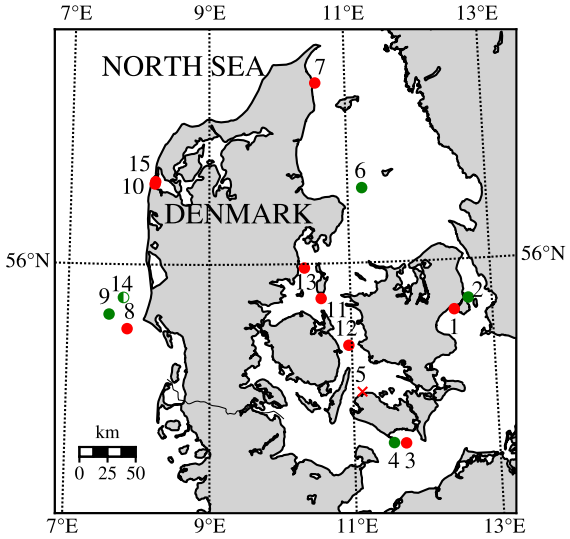

Figure 1: Offshore wind farm locations in Denmark as of December 2018 (operational: filled circle, under construction: half filled circle, decommissioned: cross, red color: wind farm with straight rows, green color: wind farm with curved rows); 1: Avedøre Holme (10.8 MW), 2: Middelgrunden (40.0 MW), 3: Nysted (165.6 MW), 4: Rødsand II (207.0 MW), 5: Vindeby (5.0 MW), 6: Anholt (399.6 MW), 7: Frederikshavn (7.6 MW), 8: Horns Rev I (160.0 MW), 9: Horns Rev II (209.3 MW), 10: Rønland (17.2 MW), 11: Samsø (23.0 MW), 12: Sprogø (21.0 MW), 13: Tunø Knob (5.0 MW), 14: Horns Rev III (406.7 MW), 15: Nissum Bredning Vind (28.0 MW).

These wake effects are computed by applying two different engineering wake models along with a Reynolds-averaged Navier-Stokes (RANS) model; their methodology is described in Section 2. AEP is calculated using two different wind resource cases, also elaborated on in Section 2. In Section 3, the results of applying the models to the existing curved layout of the Horns Rev II wind farm and a pseudo-straightened layout are presented and discussed. The analysis is complemented by simulating the wake effects of a single curved and straight wind turbine row layout. To conclude the results in Section 3, an analysis to quantify the impact of wake effects in different layouts on the Danish energy system is performed. The method of this analysis is added to Section 2. In this section, first the tested wind farm layouts are described.

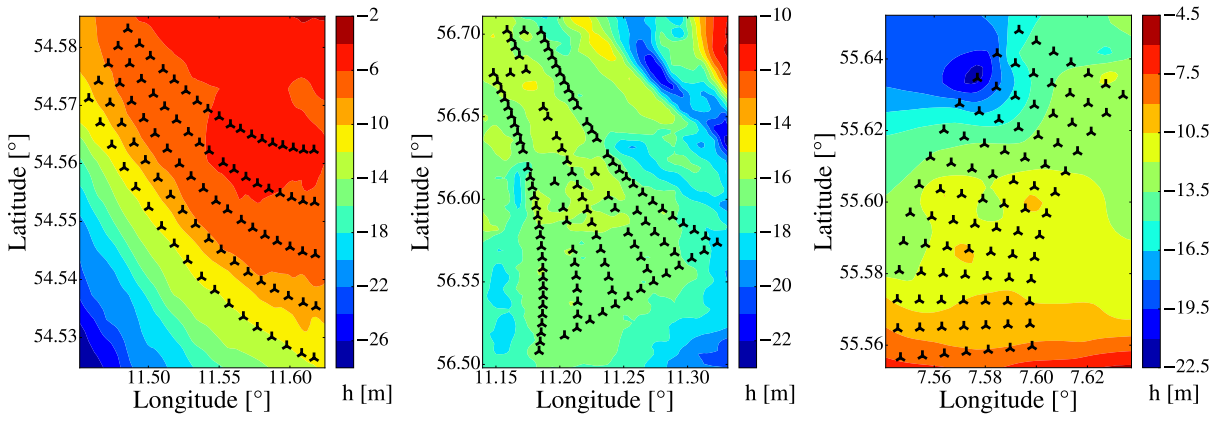

Figure 2: Sea bed contour and wind farm layouts. a: Rødsand II, b: Anholt, and c: Horns Rev II.

2. Methodology

2.1. Test cases: Wind farm layout

The test wind farm layout is based on the Horns Rev II wind farm, which consists of 7 curved rows of 13 SWT-2.3-93 wind turbines manufactured by Siemens Wind Power A/S. This wind turbine type has a rotor diameter, D, of 92.6 m, a rated power of 2.3 MW and a hub height of 68 m. The same wind turbine has been used in previous work [6] on the Lillgrund wind farm where the wind turbine hub height is 65 m. The total curvature of the Horns Rev II wind farm layout is 44.4°, see Figure 3a. The internal distances of the curved inner and outer rows are 694 m ($7.49D$) and 905 m ($9.77D$), respectively.

A comparison between wake effects of wind farm layouts with curved and straight rows is made by introducing a rectangular layout based on the Horns Rev II wind farm, with conservation of the total wind farm area. Since the Horns Rev II wind farm layout is found to accurately match with a polar coordinate system in both radial and angular direction within 1 m, see Figure 3a, the rectangular wind farm is created by averaging the internal distances. Please note that deviations of this order do not lead to measurable changes in wake effects. The spacing in the short-side (radial) direction of the pseudo-straightened wind farm is calculated by taking the average of all radial distances in the actual wind farm, i.e 545 m ($5.89D$). Since the actual wind farm is curved, two neighbouring radial wind turbine lines are not aligned in Cartesian coordinates. Therefore, the 7 distances from one radial wind turbine line to the other are averaged. Preforming this calculation for all neighbouring lines, and afterwards averaging the 12 obtained values, results in a consistent spacing in the long-side (angular) direction of 800 m ($8.64D$).

For comparison reasons, the pseudo-layout is rotated clockwise by 17.2° so the central line of both wind farm layouts coincide and thus, the power deficits of both layouts as a function of wind direction. Both the original and pseudo-layout are depicted, non-dimensionalized with the rotor diameter, in Figure 3b.

The distances in angular direction of the actual layout vary for each row, and with that the area spanned by four neighbouring wind turbines. Therefore, the comparison of the straightened layout with the original curved layout could be improved. For this purpose, only the middle row of both the curved and rectangular Horns Rev II wind farm layout are used. Internal distances between wind turbines in a single row can be easily preserved. The middle row is taken since this row represents the average spacing of the actual layout in angular direction. In Figure 3a the wind turbines used for this are highlighted in yellow. Please note that the standard deviation

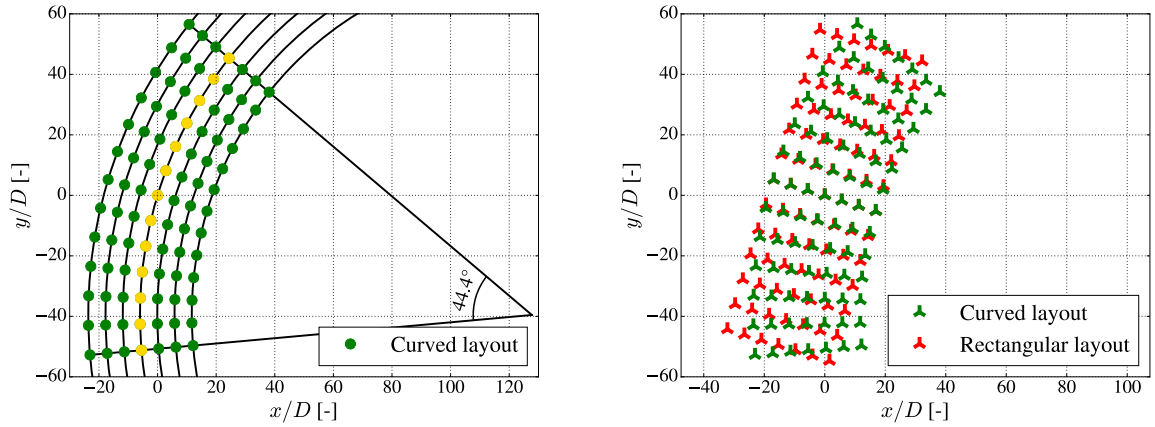

(a) (b)

Figure 3: a: Horns Rev II compared with a polar coordinate system. The wind turbine row used in the single row analysis is marked yellow. b: Actual and fictitiously straightened Horns Rev II layouts.

of this single row spacing is 0.35 m ($3.75 \cdot 10^{-3} D$), which is negligible.

An ambient stream-wise turbulence intensity, I_u, of 7.5% is used for both the RANS and engineering wake models. This represents offshore neutral conditions at hub height ($z_H = 68.0$ m) for a roughness height, z_0, of 10^{-4} m. This I_u comes from $I_u = \sigma_u/U = Au_*/[u_*/\kappa \ln(z_H/z_0)] \approx 1/\ln(z_H/z_0) \approx 0.075$, where U is the stream-wise velocity defined by the logarithmic surface layer, σ_u is the standard deviation of stream-wise velocity, $\kappa = 0.4$ is the chosen von Kármán constant, A is a constant set equal to $1/\kappa$, and u_* is the friction velocity.

2.2. Engineering wake models

Two different engineering wake models, implemented in PyWake [7], are used to calculate the wake losses in the curved and rectangular layout. PyWake is an open source, Python based, collection of engineering wake models maintained by Technical University of Denmark. The first employed engineering wake model is the NO Jensen model [8], which assumes wakes to be a top hat velocity deficit. The wake decay coefficient k_w, which represents the rate of wake expansion in downstream direction, is chosen to be 0.040, which is commonly used for offshore wind farms [9, 10]. The second employed engineering wake model is the Gaussian wake model from Bastankhah and Porté-Agel [11], which assumes a Gaussian shaped wind speed deficit. For a stream-wise turbulence intensity of 0.075 at hub height, the wake growth rate for this model is calculated to be $k^* = 0.032$ [12], which is a function of thrust coefficient and local turbulence intensity. Please note that we only use the ambient turbulence intensity. For both engineering wake models, linear and quadratic wake superpositions are modeled and presented in the study. Both wake superposition methods are used since their integrated deficit error varies differently with applied trust coefficients, C_T [13].

2.3. Reynolds-averaged Navier-Stokes

Results of the engineering wake models are verified by RANS simulations. The RANS methodology is fully described in previous work, together with a grid refinement and validation study [6, 14, 15]. Therefore only a brief summary of the numerical setup is presented here. The finite volume flow solver EllipSys3D [16, 17] is used to solve the RANS equations whereas the Reynolds-stress is modeled by the k-ε-f_P model [14], which is an extended k-ε model, developed

for wind turbine wake simulations. The numerical grid of the rectangular and curved Horns Rev II wind farm layout is a Cartesian domain with a dimension of $1200D \times 1200D \times 16D$, for the stream-wise, lateral and vertical directions, respectively. In the horizontal center of the grid, a refined domain with dimensions $117D \times 128D \times 4D$ is used to resolve the wind turbine wakes, with grid spacing not exceeding $D/8$. The flow direction is always aligned with the west-east grid lines, while the wind farm layout is rotated to simulate different wind directions. This avoids additional numerical diffusion that occurs when the flow is not aligned with the grid lines. The total amount of cells is about 75 million. The domain of the straight and curved wind turbine row has a smaller refined domain that varies with a wind direction sector. The boundary conditions are: inlet at the upstream and top boundaries at which a neutral logarithmic surface layer is set, periodic conditions at the lateral boundaries, a rough wall boundary [18] at the bottom, and an outlet condition at the downstream boundary, at which zero gradients in the normal direction are assumed. The wind turbines are modeled as Actuator Disks (AD) [19, 20] using a variable force method [15]. Rotation forces are neglected, such that we can use wind farm layout symmetry to reduce the number of necessary wind direction cases. Please note that the effect of wake rotation on the power deficit is negligible, as shown in previous work [6]. The roughness length ($z_0 = 1.42 \times 10^{-4}$ m) is used to set a total turbulence intensity of 6%, which corresponds to the stream-wise turbulence intensity of 7.5% ($I_{\text{total}} \approx 0.8 I_u$ [14]). Effects of Coriolis and thermal forces are disregarded. Previous work [21] has shown that effect of Coriolis forces can impact the wake losses in a wind farm cluster consisting of two wind farms (one with a curved, and one with a rectangular wind farm layout). In this work, we only investigate wake effects within a single wind farm, where the effect of Coriolis forces is small for neutral atmospheric conditions because the wind veer over the rotor area is in the order of a few degrees.

2.4. Wind resource cases

The AEP of both the wind farm and single row layouts is analyzed for two different wind cases. In the first case, an uniform wind speed and wind direction distribution are taken, referred to as uniform distribution (UD). In the second case, Weibull and wind direction distributions are used according to WAsP [22, 23] data, given in Table 1, referred to as non-uniform distribution (ND). WAsP is a tool for wind resource assessment, siting and energy yield calculations for wind turbines and wind farms, owned by DTU. For every wind direction sector of 30°, the Weibull distribution is given with Weibull scale parameter, A, which is proportional to the mean wind speed, and Weibull shape parameter, k, which specifies the distribution shape. The wind rose distribution is specified in wind section frequency, f. Please note that the actual wind resource case is only used to analyze the total power generation ratio between the wind farm layouts with curved and straight rows in total, whereas the other results are based on flow cases and therefore based on an uniform wind resource.

2.5. Energy system level analysis

To quantify the wake effect difference between the curved and the rectangular Horns Rev II wind farm layouts on an energy system level, simulation tool Correlations in Renewable Energy Sources (CorRES) [24] is used. The CorRES tool is used to simulate the wind generation time series from each Danish offshore wind farm by assuming that they all have either the curved or rectangular Horns Rev II wind farm power curve. It is important to note that these test cases are not meant to be realistic, as the two wind farm power curves are simply copied to all wind farm locations without rotating the wind farm power curves to resemble realistic wind farm layout orientations. Additionally, power deficits are determined with the SWT-2.3-93 characteristics only. However, comparing the two cases can show the largest expected differences in power generation due to wind farm layout for the rotation used, at the simulation locations. Current and soon to be commissioned offshore wind farms are modeled, leading to 14 simulated wind

Table 1: Non-uniform (ND) wind resource data at hub height based on a WAsP simulation, given for sectors of 30°. A is the Weibull scale parameter, k is Weibull shape parameter, and f is the wind direction sector frequency.

	0°-29°	**30°-59°**	**60°-89°**	**90°-119°**	**120°-149°**	**150°-179°**
f [%]	3.597	3.949	5.167	7.000	8.365	6.435
A [m/s]	9.177	9.782	9.532	9.910	10.042	9.594
k [-]	2.393	2.447	2.412	2.592	2.756	2.596
	180°-209°	**210°-239°**	**240°-269°**	**270°-299°**	**300°-329°**	**330°-359°**
f [%]	8.643	11.771	15.158	14.738	10.012	5.166
A [m/s]	9.584	10.515	11.399	11.687	11.637	10.088
k [-]	2.584	2.549	2.471	2.607	2.627	2.326

farms with an aggregated installed capacity of around 1.7 GW. The recently installed Nissum Bredning Vind wind farm has not been included in this analysis. The location of the 14 wind farms used in CorRES simulations are depicted in Figure 1. Generation from each wind farm is simulated on an hourly resolution. Meteorological reanalysis data from the Weather Research and Forecasting model [25] is used as input [24], giving an effective wind speed and direction for each wind farm for each analyzed hour. The curved and rectangular wind farm power curves as input for CorRES are calculated by the Gaussian engineering wake model using linear wake superposition for each wind direction. The calculated wind farm power curves are normalized with the rated power of the Horns Rev II wind farm, and they are multiplied by the rated power of each wind farm. A total of 35 meteorological years are simulated (1982-2016). The effect of wind farm wake interaction is neglected.

3. Results and Discussion

The wake effects are evaluated by normalizing the wind farm power by the wind farm power without wake losses. The undisturbed wind farm power is calculated as the integral of the power curve [6] multiplied by the amount of wind directions (360) and wind turbines considered (91 for the wind farm analysis and 13 for the single row analysis). Wind speeds ranging from 4 m/s to 25 m/s are considered. For modelling purposes, the cut-in wind speed in the engineering wake models is regulated by assuming wind turbines to be out of operation for wind speeds smaller than 4 m/s.

All results obtained with the engineering wake models and RANS model are post processed with a Gaussian filter using a standard deviation of $\sigma = 5°$ to represent the effect of wind direction uncertainty, as discussed by Gaumond et al. [26]. Through this analysis, values are obtained by averaging the results of the two engineering wake models, both applied with the two different wake superposition methods (linear and quadratic). Please note that the Gaussian engineering wake model with linear wake superposition is closest to the averages of all wake models used. All engineering wake models are included as shaded regions in Figures 4 and 5 to show their variability.

3.1. Wake effects in wind farm

For a free-stream wind speed of 8 m/s at hub height, the normalized power as a function of wind direction is given in Figure 4a, for both the curved and rectangular Horns Rev II wind farm layouts. RANS simulations are performed for a wind direction sector of about 45° around the wind direction with the largest wake effects for the rectangular wind farm (287°), with an interval of 5°. The trends in the power deficit simulated with RANS compare well with the averaged power deficit trends obtained with the employed engineering wake models. As

expected, the wake losses are highest in the aligned wind directions, which is mainly visible for the rectangular wind farm layout. This layout also shows stronger and narrower power deficits around the aligned wind directions. From Figure 4a, it can be concluded that the power of the curved wind farm layout is less sensitive to wind direction compared to the rectangular wind farm layout. In Figure 4b, the normalized power of the curved and rectangular wind farm

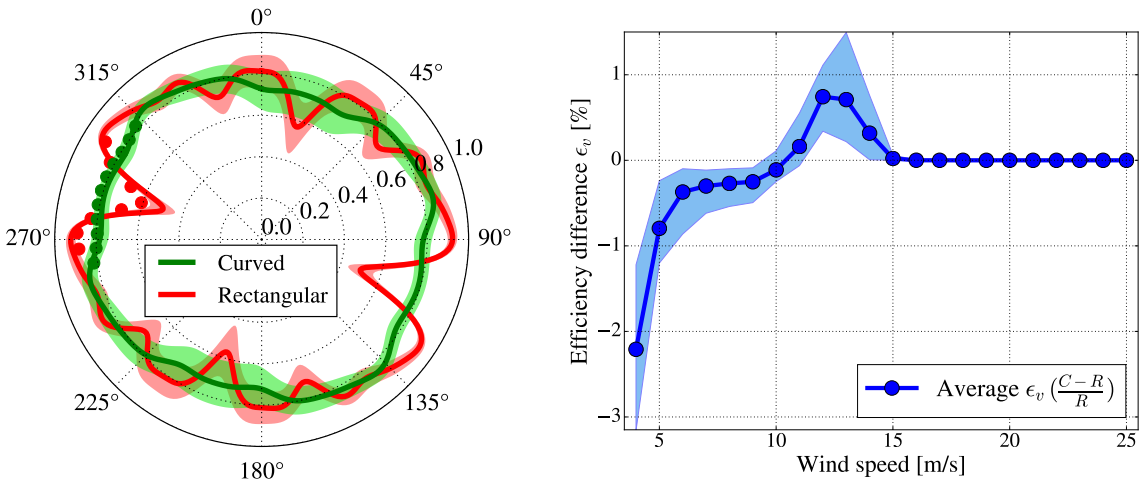

(a) (b)

Figure 4: a: Normalized power for both the curved and pseudo-straightened layout obtained with engineering wake models and RANS (dots). Both the actual and undisturbed (for normalization) wind farm power are computed for a free-stream wind speed of 8.0 m/s. b: The efficiency of the curved (C) compared with the rectangular (R) layout integrated over all wind directions, as a function of all considered wind speeds calculated by the engineering wake models. In both a and b, the results of all engineering wake models are plotted as an average (line) and spread (shaded area).

layouts, integrated over all wind directions, are compared as a function of the wind speeds, averaged for all used employed engineering wake models and wake superpositions. This is done by subtracting the rectangular layout power from the curved layout power, normalizing with the rectangular layout power; $(C - R)/R$. As a function of wind speed, this ratio is denoted with variable ϵ_v. In the lower wind speed range (below 11 m/s) the rectangular wind farm layout performs better, while in the mid wind speed range (11-15 m/s) the curved wind farm layout is favorable. Please note that in the lower wind speed range the trust coefficient C_T is high, which starts decreasing from 10 m/s [6].

In Table 2, a comparison between the curved and rectangular wind farm layout is made for the different engineering wake models used. Here, the total curved-rectangular ratio is listed for both wind distribution cases (UD and ND), where integration over all wind speeds and wind directions considered. This total ratio is denoted with ϵ. The results show that the curved wind farm layout is always performing better, with a maximum of 0.225% for the Jensen model with linear wake superposition. An AEP gain of this order is rather small. Although the wind farm layout with straight rows is better than the curved wind farm layout below 11 m/s, as shown in Figure 4b, the curved wind farm layout is favorable since the wind turbine power is higher for higher wind speeds [6]. For the non-uniform wind distribution case, where the real Weibull and wind direction frequencies are considered, the curved wind farm layout is even more favorable as the wind frequently comes from wind directions in which the rectangular wind farm layout shows the largest wake effects, see Table 1 and Figure 4b.

Table 2: AEP comparison of the wind farm layouts with curved and straight rows for both the wind farm layout and single row layout. Percent difference values ϵ are given for all engineering wake model simulation approaches and uniform (UD) and non-uniform (ND) wind speed and wind direction distributions. All wind speeds and wind directions are taken into account.

ϵ [%]	Engineering wake model			
	Jensen linear	Jensen squared	Gaussian linear	Gaussian squared
HR II farm (UD)	0.148	0.081	0.082	0.026
HR II farm (ND)	0.225	0.158	0.086	0.025
HR II row (UD)	0.125	0.003	0.089	-0.006
HR II row (ND)	0.259	0.052	0.216	0.035

3.2. Wake effects in single wind turbine row

To improve the comparison between a curved and a rectangular wind farm layout, the analysis from Section 3.1 is repeated for a single wind turbine row, where the spacings between the wind turbines within the curved and straight wind farm row are constant. The middle row of the Horns Rev II wind farm layout is taken, see Figure 3a, and compared with the middle row of the pseudo-straightened wind farm layout. For a free-stream wind speed of 8 m/s, the normalized power as a function of wind direction is given in Figure 5a, for both the curved and straight wind farm row. All employed engineering wake models applied with different wake superpositions, and their average, are given for a uniform wind speed and wind direction distribution. RANS results are added for the whole wind direction sector with an interval of 2.5°.

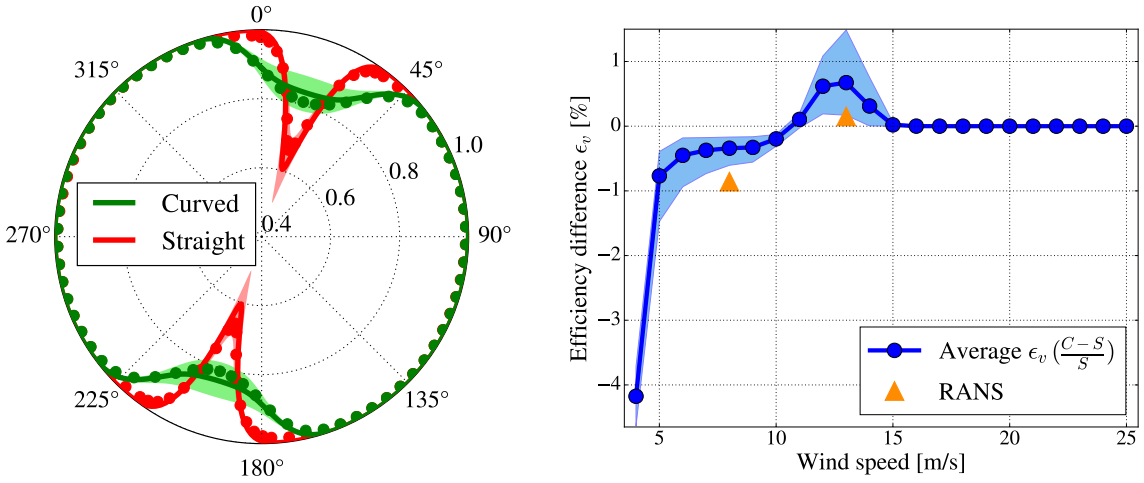

(a) (b)

Figure 5: a: Normalized power for both the curved and straight single row obtained with engineering wake models and RANS (dots). Both the actual and undisturbed (for normalization) wind farm power are computed for a free-stream wind speed of 8.0 m/s. b: The efficiency of the curved (C) compared with the straight (S) wind turbine row integrated over all wind directions, as a function of all considered wind speeds calculated by the engineering wake models. Two RANS results are shown, integrated over all wind directions, for a wind speed of 8 m/s and 13 m/s. In both a and b, the results of all engineering wake models are plotted as an average (line) and spread (shaded area).

For aligned wind directions, the straight row layout generates less power compared to the

curved row layout. The curved row layout shows wake losses to be spread out over a larger range of wind directions. For both the curved and straight row, RANS simulations are consistent with the power deficit results averaged over all employed engineering wake models, for all wind directions. Remarkably, the curved row layout performs differently in both perpendicular wind directions using RANS, see Figure 5a (hard to see). For a free-stream wind speed of 8 m/s, the normalized power is 99.4% and 99.1% in wind directions 287.2°(convex side) and 107.2°(concave side), respectively. For these flow cases, the engineering wake models do not show wake effects.

In Figure 5b, the ratio between the curved and straight row layout integrated over all wind directions is given as a function of wind speed. Here, RANS simulations are added for both 8 m/s and 13 m/s. As a function of the wind speed the power ratio is given as $(C - S)/S$ and is denoted with ϵ_v. Again, for low wind speeds (below 11 m/s) the straight row layout is performing better while the curved wind farm layout dominates for speeds ranging from 11 m/s to 15 m/s. The added RANS simulations are in line with this as the signs correspond, but show lower values for the percent difference ϵ_v. The ratio between the AEP of the curved and straight row layout, ϵ, are added to Table 2, for both wind cases (UD and ND) and both employed engineering wake models and wake superpositions. Most models show that the curved row layout performs better with a maximum of 0.259%. However, this AEP gain is again negligibly small.

Wake effects differ from wind turbine to wind turbine in a row. Both the curved and straight layout show different wake effects for particular wind directions, as illustrated in Figure 5a. For both the curved and straight row layout, the normalized power for every wind turbine in the row is given in Figure 6a and 6b, respectively. The Gaussian engineering wake model with linear wake superposition is used, and the normalized powers are calculated for a wind speed of 8 m/s. Five different wind directions are considered starting from the aligned wind direction (17.2°). Intervals used for the straight and curved row are 2.0° and 7.5°, respectively, see Figure 6c.

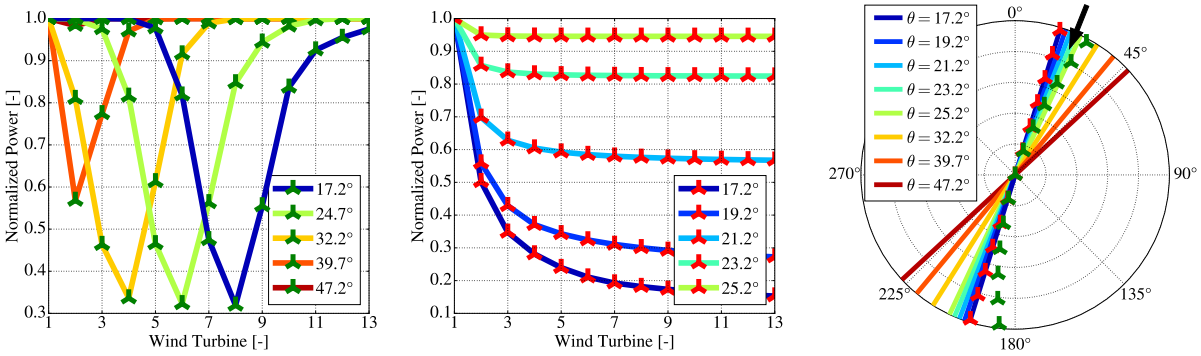

(a) (b) (c)

Figure 6: Normalized power output per wind turbine for different wind directions. Computed with Gaussian engineering wake model with linear wake superposition for a wind speed of 8 m/s. a: Curved row and b: Straight row. c: Curved and straight row with the analyzed wind directions, with northern wind.

In both layouts, the front wind turbine is generating at its maximal power, whereas the other wind turbines experience wake effects. For the straight row layout, a small deviation from the aligned wind direction results in a significant power increase for all remaining wind turbines. This generated power converges to a certain value further downstream. For the curved row layout, a large deviation (15°) from the aligned wind direction still results in a nearly unchanged integrated normalized power generation over all wind turbines. However, the concentration of wind turbines experiencing wake losses shifts significantly towards the first turbine in the row, see Figure 6a. A similar effect for a curved wind farm (Rødsand II) has been observed by Hansen

et. al [27]. Wind turbines in the curved row interfere in a larger range of wind directions. This explains the spreading of normalized power over wind directions in a curved row layout compared to a straight row layout.

3.3. Effects on energy system level

Figure 7 depicts the wind farm power of one rectangular and one curved wind farm layout (located at Horns Rev II), normalized by the rated wind farm power, as a function of the hourly mean wind speed, simulated with CorRES (Section 2.5), for one simulation year (2016). It can be seen that the normalized power of the curved wind farm layout shows less variability in the generation output for a given wind speed compared to the rectangular wind farm layout because the power variation with wind direction of the curved wind farm layout is significantly lower compared to the rectangular wind farm layout, as shown previously in Figure 4a. Please note that a simple generic storm shut down model was implemented in CorRES, which explains the low generation values at high wind speeds.

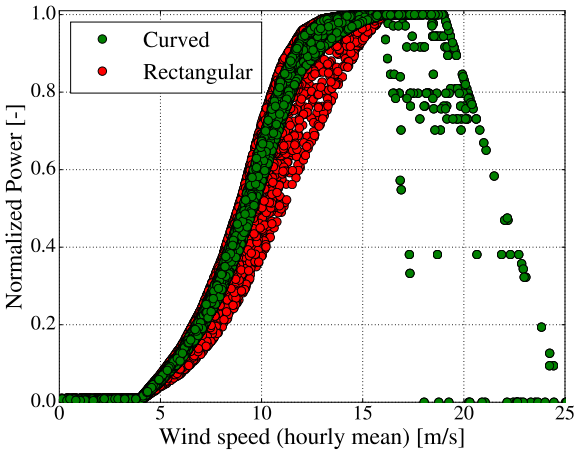

Figure 7: Hourly mean wind speed and generation output of an example offshore wind farm (located at Horns Rev II) in the rectangular and curved wind farm simulation cases for one simulation year (2016).

Table 3 lists the ramp standard deviation (SD) of rectangular and curved wind farm layouts at three different locations; Rødsand II, Anholt and Horns Rev II. Ramp SD is the SD calculated from the first difference of the hourly power output, for example from $\Delta p_t = p_t - p_{t-1}$, where p_t is generation at hour t. It can be seen that the hourly ramp SD is different for every location, where the curved wind farm layout shows an approximately 7% lower hourly ramp SD at all 14 simulated locations. This means that when the wind direction changes in time, the curved wind farm layout results in less ramping in the power output of a wind farm. A lower variability in wind generation output puts less strain on the overall energy system, as less balancing from other generation units is required [28]. Since the hourly ramp SD difference is significant, it is of interest to perform additional research on the effect of the layout on the induced strain on the overall energy system, rather than mainly focusing on AEP gain. It can be seen that the statistics in Table 3, namely capacity factor (CF) and the SD of the generation (for example of p_t), are very similar in the two test cases. This shows that the lower ramp SD does not come at the expense of for instance the lower energy yield of the wind farm.

Table 3: Statistics of the rectangular (R) and curved (C) Horns Rev II wind farm layout test cases using 35 years of simulated hourly data for three simulated offshore wind farms; Rødsand II (RS II), Anholt (AH), and Horns Rev II (HR II). CF = capacity factor, SD = standard deviation.

OWPP	**CF (R)**	**CF (C)**	**SD (R)**	**SD (C)**	**Hourly ramp SD (R)**	**Hourly ramp SD (C)**	**Ramp SDs ratio (C/R)**
RS II	0.414	0.415	0.346	0.343	0.0863	0.0800	93%
AH	0.429	0.431	0.351	0.349	0.0851	0.0791	93%
HR II	0.465	0.465	0.357	0.355	0.0854	0.0794	93%

4. Conclusion

In this paper, wake effects of the Horns Rev II offshore wind farm, originally designed with curved wind turbine rows, are compared with a pseudo-straightened wind farm using different engineering wake models and RANS simulations. To improve the comparison of wake effects in both layouts, the study has been supplemented with an analysis of one wind turbine row of each layout. On plant-level, for both the Horns Rev II wind farm and single wind turbine row, engineering wake models and RANS simulations predict that the power generation of the pseudo-straightened layouts are more dependent on wind direction compared to the actual curved layouts, while the difference in AEP between the wind farm layouts is negligible. The turbine-level study shows that almost all downstream located wind tribunes in a straight row generate less power in aligned wind directions, whereas in a curved row the wake effects only influence a few wind turbines significantly. However, in a curved row significant wake effects are found for a larger wind direction sector.

The wake effects of both the curved and pseudo-straightened wind farm layouts are implemented in a time series wind generation simulation tool, CorRES, to compare their effects on the Danish energy system level. CorRES predicts that the curved wind farm layout has less variability in the energy supply on a national energy system level compared to a rectangular wind farm layout because the power generation of the curved wind farm is less dependent on wind direction than the rectangular wind farm layout. As a consequence, the hourly ramp standard deviation of the curved wind farm layout is approximately 7% less than the hourly ramp standard deviation pseudo-straightened of the wind farm layout. As a result of that, less stress is put on an energy system. Thus, this study reveals that wind farms consisting of curved rows are better than wind farms containing straight rows. In future work, a cost model regarding a decrease in power fluctuation with wind direction should be developed, which could then be used in wind farm layout optimization.

References

[1] 2018 Offshore wind in europe key trends and statistics 2017 Tech. rep. Wind Europe URL `https://windeurope.org/wp-content/uploads/files/about-wind/statistics/WindEurope-Annual-Offshore-Statistics-2017.pdf`
[2] Hirth L, Ueckerdt F and Edenhofer O 2015 *Renewable Energy* **74** 925–939
[3] Barthelmie R J, Frandsen S T, Nielsen N M, Pryor S C, Réthoré P E and Jørgensen H E 2007 *Wind Energy* **10** 217
[4] Feng J and Shen W Z 2017 *Energy Conversion and Management* **148** 905–914
[5] EMODnet Bathymetry accessed November 2018 URL `http://portal.emodnet-bathymetry.eu/`
[6] van der Laan M P, Sørensen N N, Réthoré P E, Mann J, Kelly M C, Troldborg N, Hansen K S and Murcia J P 2015 *Wind Energy* **18** 2065
[7] PyWake URL `http://doi.org/10.5281/zenodo.2562662`
[8] Katic I, Højstrup J and Jensen N O 1987 *European wind energy association conference and exhibition* (A. Raguzzi)

[9] Nygaard N G 2014 *Journal of Physics: Conference Series* vol 524 (IOP Publishing) p 012162
[10] Cleve J, Greiner M, Enevoldsen P, Birkemose B and Jensen L 2009 *Wind Energy: An International Journal for Progress and Applications in Wind Power Conversion Technology* **12** 125–135
[11] Bastankhah M and Porté-Agel F 2014 *Renewable Energy* **70** 116–123
[12] Niayifar A and Porté-Agel F 2015 *Journal of physics: conference series* vol 625 (IOP Publishing) p 012039
[13] Machefaux E, Larsen G C and Leon J M 2015 *Journal of Physics: Conference Series* vol 625 (IOP Publishing) p 012037
[14] van der Laan M P, Sørensen N N, Réthoré P E, Mann J, Kelly M C, Troldborg N, Schepers J G and Machefaux E 2015 *Wind Energy* **18** 889
[15] van der Laan M P, Sørensen N N, Réthoré P E, Mann J, Kelly M C and Troldborg N 2015 *Wind Energy* **18** 2223
[16] Sørensen N N 1994 *General purpose flow solver applied to flow over hills* Ph.D. thesis DTU
[17] Michelsen J A 1992 Basis3d - a platform for development of multiblock PDE solvers. Tech. rep. DTU
[18] Sørensen N N, Bechmann A, Johansen J, Myllerup L, Botha P, Vinther S and Nielsen B S 2007 *Journal of Physics: Conference series* **75** 1
[19] Mikkelsen R 2003 *Actuator Disc Methods Applied to Wind Turbines* Ph.D. thesis DTU
[20] Réthoré P E, van der Laan M P, Troldborg N, Zahle F and Sørensen N N 2013 *Wind Energy* Pub. online
[21] van der Laan M P, Hansen K S, Sørensen N N and Réthoré P E 2015 *Journal of Physics: Conference Series* **524** 1
[22] Troen I and Petersen E L 1989 *European Wind Atlas* (Risø National Laboratory, Roskilde)
[23] Wasp URL `http://wasp.dk/`
[24] Koivisto M, Das K, Guo F, Sørensen P, Nuño E, Cutululis N and Maule P 2018 *Wiley Interdisciplinary Reviews: Energy and Environment* e329
[25] Peña A and Hahmann A N 2017 30-year mesoscale model simulations for the noise from wind turbines and risk of cardiovascular disease project Tech. Rep. DTU Wind Energy-E-Report-0055(EN) DTU Wind Energy
[26] Gaumond M, Réthoré P E, Ott S, Peña A, Bechmann A and Hansen K S 2014 *Wind Energy* **17** 1169–1178
[27] Hansen K S, Réthoré P E, Palma J, Hevia B, Prospathopoulos J, Penã A, Ott S, Schepers G, Palomares A, van der Laan M P and Volker P 2015 *Journal of Physics: Conference Series* **625** 1
[28] Koivisto M, Maule P, Nuño E, Sørensen P and Cutululis N 2018 *Journal of Physics: Conference Series* vol 1104 (IOP Publishing) p 012011